Magnetic hysteretic phenomena in multiferroic $HoMnO_3$ single crystals and polycrystals with nano- and micrometer particle size

2008 J. Phys.: Condens. Matter 20 325241

(http://iopscience.iop.org/0953-8984/20/32/325241)

J. Phys.: Condens. Matter **20** (2008) 325241 (7pp) doi:10.1088/0953-8984/20/32/325241

Magnetic hysteretic phenomena in multiferroic $HoMnO_3$ single crystals and polycrystals with nano- and micrometer particle size

E Galstyan[1], B Lorenz[1], K S Martirosyan[2], F Yen[1], Y Y Sun[1], M M Gospodinov[3] and C W Chu[1,4,5]

[1] Department of Physics and Texas Center for Superconductivity, University of Houston, Houston, TX 77204-5002, USA
[2] Chemical and Biomolecular Engineering Department, University of Houston, Houston, TX 77204-5002, USA
[3] Institute of Solid State Physics, Bulgarian Academy of Science, 1784 Sofia, Bulgaria
[4] Lawrence Berkeley National Laboratory, 1 Cyclotron Road, Berkeley, CA 94720, USA
[5] Hong Kong University of Science and Technology, Hong Kong, People's Republic of China

E-mail: egalstyan@uh.edu

Received 22 April 2008, in final form 2 July 2008
Published 21 July 2008
Online at stacks.iop.org/JPhysCM/20/325241

Abstract

We report on the magnetic properties of multiferroic hexagonal $HoMnO_3$ single crystals and polycrystalline samples with micrometer and nanometer particle size. We have studied the in-plane and out-of-plane magnetization of $HoMnO_3$ single crystals under low applied magnetic fields in the temperature range below $T_{Néel} = 72$ K and observe the bifurcation of zero-field-cooled and field-cooled curves at the Mn spin reorientation transition temperature at 34 K. In addition, the *c*-axis magnetization shows a ferrimagnetic-like behavior which may relate to the magnetic Ho^{3+} and Mn^{3+} domain boundary structures and sensitively respond to changes of the magnetic structure such as spin rotations at the phase transitions near 5 and 34 K. We also studied the particles' size dependent magnetic behavior in the $HoMnO_3$ polycrystalline samples and observe the presence of a net magnetic moment at the surface due to the large surface/volume ratio. Below the Ho^{3+} ordering temperature of 5 K, magnetization curves as a function of applied magnetic field, in contrast to those for the single crystal, show hysteresis behavior with coercivity, which increases with diminishing particle size.

1. Introduction

Multiferroics [1–3] are a class of materials with great promise for design and manufacturing of multifunctional electric devices. They are noteworthy for their unique and strong coupling of electric, magnetic, and structural order parameters, leading to coexistence of ferroelectricity, magnetism, and/or ferroelasticity. In particular, multiferroic magnetoelectrics maintain a magnetization and dielectric polarization, which can be modulated and activated by electric and magnetic fields, respectively [4]. For this reason, the mutual control of electric and magnetic properties is of significant interest for applications in magnetic storage, sensors, and spintronics [5, 6].

The hexagonal $HoMnO_3$ is a prototype multiferroic in which the order parameters are naturally coupled through the Ho–Mn exchange and anisotropy interactions [4, 7, 8]. The Ho–O displacements give rise to a ferroelectric moment ($T_C = 875$ K) along the *c*-axis and the Mn^{3+} moments order at the Néel temperature $T_N \sim 72$ K, followed by a Mn^{3+} spin rotation transition at $T_{SR} = 34$ K that is accompanied by a partial ordering of the Ho spins along the *c*-direction [4, 5, 7–9]. The magnetic moment of the Ho^{3+} ion is completely ordered below $T_{Ho} \sim 5$ K combined with another rotation of Mn

spins in the basal plane [8]. The complete magnetic structure in all subsequent phases is not resolved yet, and it is further complicated because the Mn moments occupy a fully frustrated triangular lattice.

In addition to the complex physical properties of single crystals, the physical parameters of polycrystalline multiferroic materials are also influenced by their particle size. The macroscopic properties of materials are strongly altered when their size is significantly reduced. Collective phenomena such as magnetism and ferroelectricity change when the particle size is reduced—the influence of surface and grain boundaries become larger and eventually no long-range order is possible anymore. Experiments have revealed that the particle size plays an important role in the ferroelectric phase transition and dielectric properties of ferroelectric materials [10, 11]. Antiferromagnetic (AFM) nanoparticles have also received vast attention due to the imbalance of spins 'up' and 'down' at and near the surface [12], and their potential for showing reversal of magnetization by quantum tunneling [13]. In multiferroics, the enhancement of magnetic parameters with decreasing particle size could be favorable for the technological application of magnetoelectronics.

We present here a comprehensive study of the magnetic properties of multiferroic $HoMnO_3$ measured on single crystals and polycrystalline samples. We demonstrate that magnetic irreversibility (*spontaneous magnetization*) in single crystals appears in the zero-field-cooled (ZFC) and field-cooled (FC) temperature-dependent magnetization curves measured at low applied magnetic fields. Moreover, we observed the signature for ferrimagnetism, which may arise from the domain boundary structure and/or from the two interacting magnetic Ho^{3+} and Mn^{3+} sublattices. To ensure that this effect is intrinsic, we detected the same phenomenon on different $HoMnO_3$ single crystals prepared by various methods. We have also studied the influence of nano/microsize particles of $HoMnO_3$ as-prepared polycrystalline materials on magnetic parameters and show the systematic changes of coercive field (H_C) and remanent moment (M_{rem}) with diminishing particle size.

2. Experimental details

Single crystals of $HoMnO_3$ have been grown via the high temperature flux method [14] and in a floating zone furnace. As a reference sample, polycrystalline $HoMnO_3$, marked as P_{MR}, was prepared by grinding a single crystal. Polycrystalline $HoMnO_3$ specimens with nano and micrometer size particles, denoted as P_N and P_M samples, were synthesized at 1000 °C by a novel self-sustaining one step process, carbon combustion synthesis of oxides (CCSO) [15–17]. The product particle size can be controlled with increasing carbon content in the reactant mixture and oxygen concentrations. The carbon used in the CCSO is not incorporated into the product and is emitted as a gas from the sample. The carbon content of the as-synthesized product was determined by a carbon analyzer (Leco, WR-112). The final fine-powder products were cold-pressed into pellets for magnetic and dielectric measurements. Phase identification and crystal structure investigation were carried out using x-ray diffraction (XRD). Microstructural observations were performed using scanning electron microscope (SEM). The dielectric constant was measured by the high precision capacitance bridge AH 2500A (Andeen Hagerling) at 1 kHz in a physical property measurement system (PPMS) for temperature control. Magnetic susceptibility data were obtained with a superconducting quantum interference device (SQUID) magnetometer.

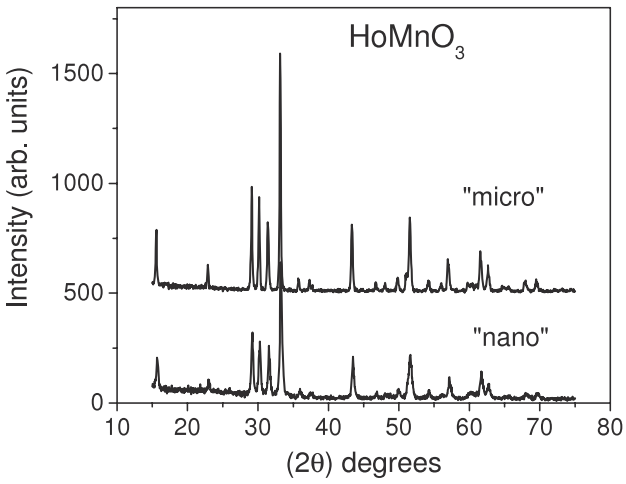

Figure 1. Powder x-ray diffraction pattern of as-prepared $HoMnO_3$ samples with nano and micrometer size particles.

3. Results and discussion

3.1. $HoMnO_3$ polycrystalline samples

The observed x-ray diffraction peak patterns (figure 1) of $HoMnO_3$ as-prepared P_M and P_N powders could be indexed to the hexagonal structure (space group: $P6_3cm$) with lattice constants of $a{:}c = 6.137(1){:}11.407(4)$ Å and $6.130(0){:}11.394(1)$ Å, respectively. These lattice parameters within the limits of uncertainty are in good agreement with results for ceramic $HoMnO_3$ synthesized by the solid state reaction technique [18, 19]. The XRD and SEM analysis of P_M and P_N powders show the complete conversion to a single-phase product without any trace of impurity phases. SEM measurements (figure 2) indicate the well-defined grains with pronounced grain boundaries in both as-prepared materials. The average size of P_N, P_M, and P_{MR} particles as determined from the SEM images were noted to be ∼80 nm, ∼1 μm, and ∼10 μm, respectively. The calculated value of the grain diameter (D) of nanoparticles from the width $\beta(= \Delta 2\theta_{1/2})$ in XRD peaks, employing a Debye–Scherer relation [20] $D = 0.9 * \lambda/(\beta * \cos\theta)$, where λ is the wavelength and θ is the angle of diffraction, yields about 30 nm. This indicates that the particles observed by SEM are composed of several nanocrystallites. The difference in microstructure of as-prepared P_M and P_N specimens demonstrates that the CCSO technique can very efficiently adjust the size of grains. In addition, the carbon analysis of as-synthesized powders indicated that the concentration of the residual carbon was less than 0.07 wt%.

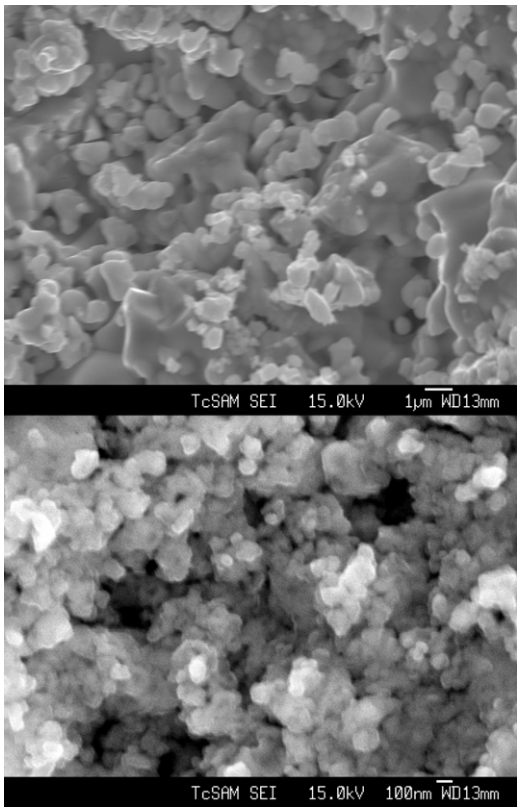

Figure 2. SEM image of as-prepared $HoMnO_3$ samples with micrometer (top) and nanometer (bottom) size particles.

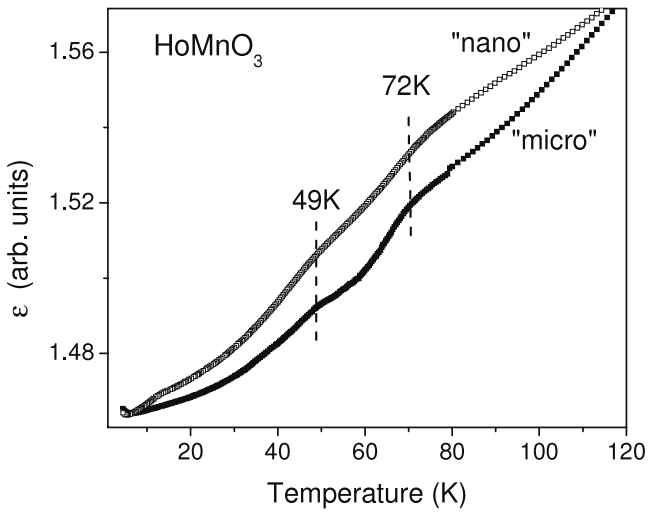

Figure 3. The temperature dependence of dielectric constant of $HoMnO_3$ samples with nano and micrometer size particles.

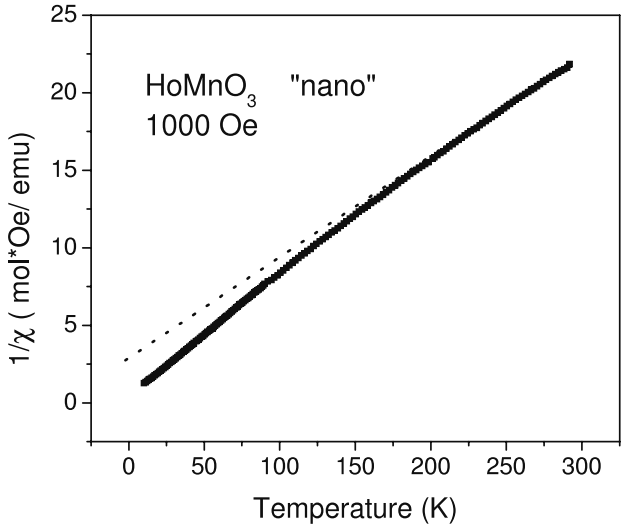

Figure 4. Temperature-dependent inverse magnetic susceptibility of $HoMnO_3$ sample with nanometer size particles. The dashed line indicates the Curie–Weiss high temperature extrapolation.

In order to unambiguously verify the presence of the previously observed magnetic phases in our as-prepared $HoMnO_3$ polycrystalline samples, we first performed the dielectric measurements. It was demonstrated recently that the major magnetic phase transitions in $HoMnO_3$ are easily detected in characteristic anomalies of the dielectric constant [7]. The temperature-dependent dielectric constant $\varepsilon(T)$ of the P_M and P_N samples at zero magnetic field is shown in figure 3. The change of slope in the $\varepsilon(T)$ plot at 72 K, which corresponds to the AFM ordering of $HoMnO_3$, is in good agreement with published results for single crystals [7, 21]. It is worth noting that the onset of AFM order of Mn^{3+} at $T_N = 72$ K is not observable from $M(T)$ measurements because of the large paramagnetic contribution of Ho^{3+} magnetic moment ($\mu_{eff} = 10.4\ \mu_B$) that masks the subtle change of magnetization [8, 14]. The other anomaly at $T_{SR} = 49$ K, which is defined also as a change of the $\varepsilon(T)$ slope, is presumably associated with the reorientation of Mn^{3+} spins and the change of the magnetic symmetry from $P6_3cm$ to $P\underline{6}_3c\underline{m}$ [4, 7, 9]. This anomaly is not as sharp as compared with single crystal data due to the polycrystalline nature of the present samples and their random particle orientation. The T_{SR} values observed earlier in $HoMnO_3$ single crystals and ceramic materials vary between 33 and 45 K, depending on the sample quality and preparation method [7, 9, 19].

The inverse magnetization, $\chi^{-1} = H/M$, of the P_N sample under applied magnetic field of 1000 Oe over a large temperature range is shown in figure 4. The reciprocal susceptibility has a linear dependence above 180 K, similar to the data obtained for P_M and P_{MR} specimens and it reveals a Curie–Weiss behavior, with an effective paramagnetic moment of 10.6 μ_B for both P_N and P_M materials. This calculated value is slightly smaller than the $\mu_{eff} = 11.5\ \mu_B$ for the $HoMnO_3$ single crystal [14]; however, it is close to $\mu_{eff} = 10.8\ \mu_B$ observed for the P_{MR} sample. The estimated value of the Curie–Weiss temperature for P_M and P_N specimens of $\theta = -17$ and -24 K, respectively, are close to earlier reported data for $HoMnO_3$ polycrystalline material [19]. The low θ in comparison with single crystal data ($\theta = -117$ K for the c-axis susceptibility) is the result of the average magnetic response from highly anisotropic, randomly oriented grains in polycrystalline samples [14]. Due to the high paramagnetic contribution of the Ho^{3+}, the level of frustration, which is determined by $|\theta|/T_N$ ratio, appears to be much smaller than

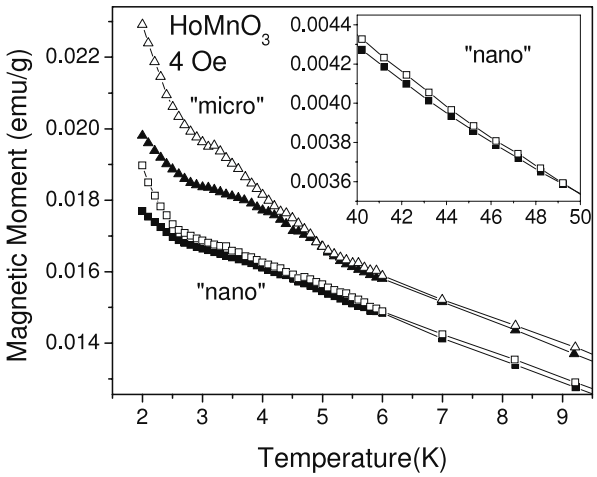

Figure 5. ZFC (solid symbols) and FC (open symbols) curves for $HoMnO_3$ samples with nano (square symbols) and micrometer (triangle symbols) size particles. Inset: magnetization of nanoparticles in temperature range from 40 to 50 K.

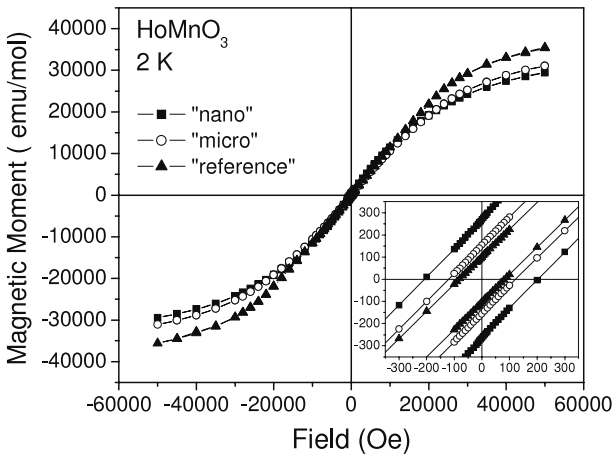

Figure 6. $M(H)$ plot at 2 K for $HoMnO_3$ with nano and micrometer size particles and reference samples. Inset: magnetization in range -350 Oe $< H <$ 350 Oe.

the value of ∼10 for $RMnO_3$, where R is a nonmagnetic element [18].

The temperature dependencies of magnetization of P_M and P_N samples taken in ZFC and FC regimes at $H = 4$ Oe are shown in figure 5. The magnetization below the Ho^{3+} AFM ordering temperature ($T_{Ho} \sim 5$ K) significantly depends on the cooling conditions (i.e., whether the sample is cooled in a field or not). Moreover, similar to the data obtained for a single crystal, as shown later, the small bifurcation of ZFC and FC curves is observable at the Mn^{3+} spin rotation temperature for the P_N sample at $T_{SR} = 49$ K (figure 5 inset, and figure 3), where Ho^{3+} becomes partially AFM ordered [9, 14]. As discussed below, the difference between ZFC and FC curves in polycrystalline samples is related to surface effects of the particles, while in single crystals this behavior arises due to the domain boundary structures. Generally, for AFM structures, especially the nanosized system, the exchange interaction between surface atoms of neighboring particles is expected to play an important role [12, 22, 23]. The imbalance in the number of spins 'up' and 'down' that occurs at the surface of the particles is the origin of a net magnetic moment below the Néel temperature [12]. This incomplete spin compensation that is possible in AFM-ordered materials becomes measurable only in small AFM systems, where the long-range AFM order is frequently interrupted at the particle surfaces.

The sizable effect on P_N, P_M, and P_{MR} samples is well observed from isothermal magnetization data at 2 K (figure 6), namely, the open hysteresis loop with $H_C = 200$, 110, and 80 Oe, respectively, which exhibits a weak-ferromagnetic-like character. Note that remarkable hysteresis loop at 2 K for a $HoMnO_3$ single crystal were not found within the error limits of the data [21]. The presence of H_C in granular materials is an indication of deviation from AFM alignments of the surface spin. In small structures, the surface-to-volume ratio becomes very large with decreasing particle size, enhancing the tangible contribution to the particle's overall magnetization by uncompensated spins at the surface [22, 23]. In addition to the major reason, the surface effect, the finite-size of particles also may contribute to the variation of H_C. In general, the coercive forces of polycrystalline ferromagnetic (FM) particles are expected to increase as the particle size decreases, at least until the particle approaches the critical size for single domain behavior [24]. In the single domain state the particle becomes magnetically harder than in the multidomain state, resulting into higher H_C. For AFM particles the observed similar trend of H_C is much more complex due to interaction between AFM cores and weak-ferromagnetic-like ordered shell, as well as the surface effect with possible spin clusters and single domain state on boundaries with diminishing of particles size [22, 23, 25, 26]. Moreover, the surface spin reorientation may also be affected by interparticle interaction. These, in turn, depend on type of interaction, the particle arrangement, and surface microstructure.

3.2. *$HoMnO_3$ single crystal*

The thermal evaluation of the magnetization of a $HoMnO_3$ single crystal with applied low magnetic field along the c-axis and in the (ab)-plane is shown in figure 7. Similar to earlier reported results [14], we observed that the in-plane ($H \parallel ab$-plane) susceptibility value is larger than the out-of-plane ($H \parallel c$-axis) one, the origin of which is not yet clear. As mentioned above for polycrystalline materials, the absence of the expected magnetic anomaly in $M(T)$ curves near $T_N = 72$ K is due to the large paramagnetic contribution of Ho^{3+}, which dominates through the temperature range above 5 K and masks the magnetization anomaly at the Néel temperature when the Mn^{3+} spins become AFM ordered [8, 14]. However, at lower temperature, at least two distinct anomalies are clearly detected. The first, a step-like drop in the c-axis magnetization at around 34 K, is accompanied by a splitting of ZFC and FC curves (figure 7, inset). At $T_{SR} = 34$ K, all spins of the Mn^{3+} rotate by 90° in the basal plane and, as shown in earlier reports [9, 14], the Ho^{3+} moments along the c-axis order partially as a result of strong correlation and coupling between Mn and Ho moments. Since the net moment inside the

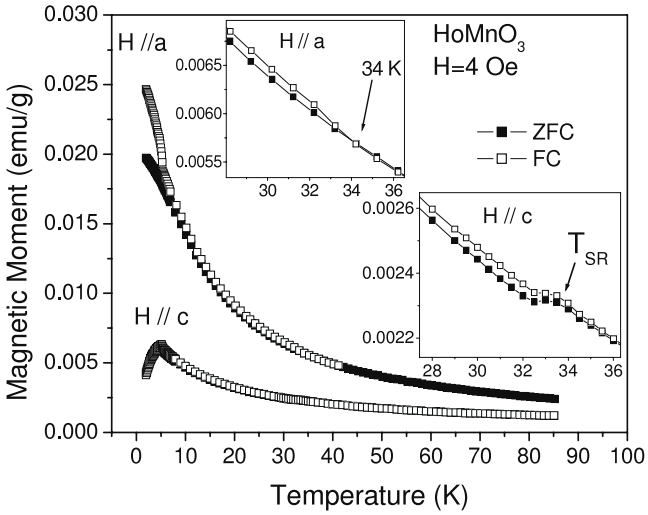

Figure 7. Temperature-dependent magnetization measurements of $HoMnO_3$ single crystal under a low magnetic field of 4 Oe applied along *c*-axis and (*ab*)-plane. Inset: ZFC (solid symbol) and FC (open symbol) curves in expanded scale.

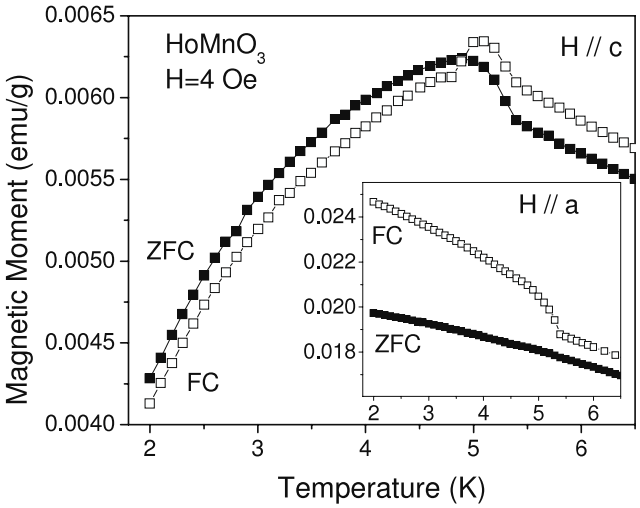

Figure 8. ZFC (solid symbol) and FC (open symbol) magnetization curves of $HoMnO_3$ single crystal at low temperature range under applied magnetic field of 4 Oe along *c*-axis and, inset, (*ab*)-plane.

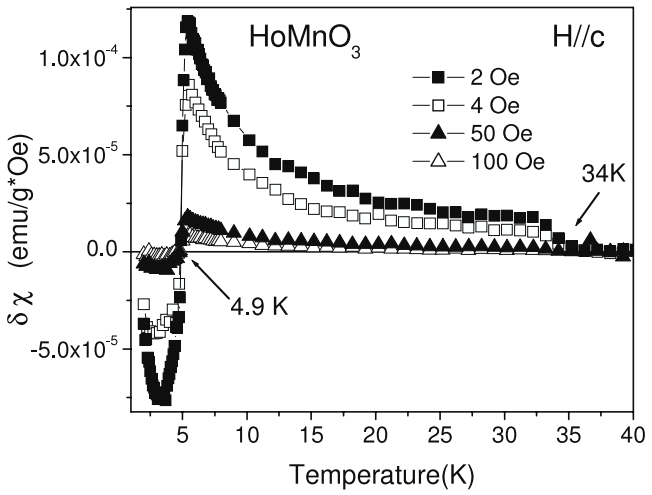

Figure 9. Susceptibility $\delta\chi$ as defined by subtracting of ZFC from FC curves ($\delta\chi = \chi_{FC} - \chi_{ZFC}$) for $HoMnO_3$ single crystal under different magnetic fields applied along *c*-axis.

perfect AFM domain is zero the observed bifurcation of ZFC–FC curves below 34 K perhaps originates from the spontaneous alignment of random magnetic Ho and/or Mn moments in domain boundaries. The onset of irreversibility phenomena, which is defined as the splitting of ZFC and FC curves at or below the Néel temperature ($T_{irr} \leqslant T_N$), has also been observed in other multiferroic hexagonal manganites such as $RMnO_3$ (R = Er, Yb, Tm, Lu, and Y), showing a similar frustrated magnetic order as in $HoMnO_3$ [8, 27, 28]. Since the net moment inside the perfect AFM domain is zero the observed bifurcation of ZFC–FC curves below 34 K, perhaps originates from the spontaneous alignment of random magnetic Ho and/or Mn moments in domain boundaries. The onset of irreversibility phenomena, which is defined as the splitting of ZFC and FC curves at or below the Néel temperature ($T_{irr} \leqslant T_N$), has also been observed in other multiferroic hexagonal manganites such as $RMnO_3$ (R = Er, Yb, Tm, Lu, and Y), showing a similar frustrated magnetic order as in $HoMnO_3$ [8, 27, 28]. In the case of $HoMnO_3$ for magnetic fields above 100 Oe applied along the *c*-axis, both ZFC and FC curves collapse and irreversibility is not observable presumably due to the strong paramagnetic contribution of Ho moment and/or the saturation of the spontaneous moments supposedly sitting in domain walls. The second *c*-axis magnetization anomaly at low temperature (figure 8) can actually be separated into two subsequent transitions at 5.1 and 4.8 K as was previously suggested from dielectric and specific heat measurements [29]. The first transition is associated with the complete AFM ordering of Ho^{3+} moments with a significant increase of the Ho sublattice magnetization [9], while the second one is presumably attributed to another rotation by 90° of Mn spins triggered by the increase of the Ho moment and their mutual coupling [8, 12]. With respect to the $M(T)$ behavior in low magnetic fields, in addition to the onset of irreversibility at $T_{SR} = 34$ K, we make the following new observation in the low temperature range: on cooling from temperatures above T_{SR} or T_N in a magnetic field oriented parallel to the *c*-axis of the $HoMnO_3$ crystal, the susceptibility is first higher in the case of a FC measurement as compared with that of ZFC, but upon further cooling below 4.8 K, the FC magnetization becomes smaller than the ZFC curve (figure 8). This behavior is intrinsic and has been observed for the $HoMnO_3$ single crystals prepared by different methods such as flux and floating zone growth techniques. The difference between the FC and ZFC susceptibilities ($\delta\chi = \chi_{FC} - \chi_{ZFC}$) decreases with increasing field and vanishes above 100 Oe (figure 9). Such a phenomenon is typical for ferrimagnetic structures, although the $HoMnO_3$ single crystal does not show a visible magnetic hysteresis loop even below T_{Ho} (figure 10), which is consistent with earlier published results [21], where it was concluded that the residual magnetization, if any, is less than 0.002 μ_B per formula unit. Instrumental resolution may not be enough to detect such a small hysteresis. We assume

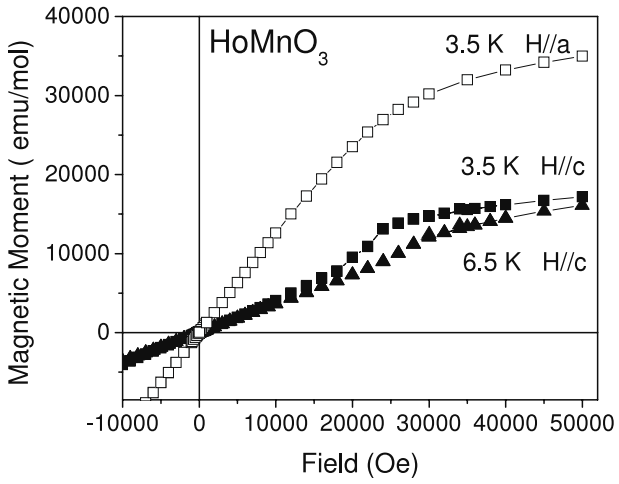

Figure 10. In-plane (open symbol) and out-of-plane (solid symbols) magnetization $M(H)$ plot of $HoMnO_3$ single crystal at 3.5 and 6.5 K.

that the nature of observed ferrimagnetic-like behavior under an applied small out-of-plane magnetic field in $HoMnO_3$ single crystals is related to the different temperature dependence of inequivalent Ho^{3+} and Mn^{3+} magnetic subsystems that are oppositely aligned in the AFM domain walls. A magnetization reversal, in general, is frequently observed in ferrimagnetic systems, in which two magnetic subsystems are strongly AFM coupled. In $HoMnO_3$, however, the observed effects are small and only observable at low magnetic fields. We therefore attribute the observed effects to a ferrimagnetic coupling of the c-component of the Mn spins and the Ho moments in the AFM domain boundaries. Below T_{SR} a net magnetic moment arises in the domain boundary and it is first aligned with the external field, but it is reversed at 5 K due either to the increase of the Ho sublattice magnetization or to a reversal of the c-component of the Mn spins. This could explain the unusual fact that the FC data are lower than the ZFC magnetization at low temperatures. Another scenario possibly explaining the observed ferrimagnetic-like behavior in $HoMnO_3$ single crystals is associated with the intrinsic properties of the Ho^{3+} magnetic subsystem: along the c-axis, the AFM order of 2/3 of the Ho spins sets in at $T_{SR} = 34$ K, while the remaining Ho moments completely order at 5.1 K [9, 14]. Hence, a weak ferrimagnetism could arise from the competition of AFM-ordered Ho magnetic sublattices with different values of the magnetic moment.

4. Conclusion

We have studied the multiferroic hexagonal $HoMnO_3$ single crystal and polycrystalline samples and observed the hysteretic magnetic anomalies associated with domain boundary structures in single crystals and surface effects of microsize and nanosize particles in polycrystalline materials. The influence of nano/microsize particles on the magnetic properties of $HoMnO_3$ shows a sizable difference in the temperature and field dependence of the magnetization below 5 K, where Ho spins become antiferromagnetically ordered and magnetic parameters, such as coercive field and remanent moment, increase with diminishing particle size. It is well established that surface anisotropies dominate magnetic behavior in small particles. Thus, we believe that the enhancement of magnetization is primarily related to the contribution of uncompensated spins at the surface of particles.

We also investigated the in-plane and out-of-plane magnetization properties of $HoMnO_3$ single crystals at low applied magnetic field. The temperature-dependent measurement reveals an unexpected bifurcation of ZFC and FC curves at 34 K, where the Mn spin rotation and partial AFM ordering of Ho moments take place. We associate this weak irreversibility behavior with net components of spontaneous Mn and/or Ho moments in the neighboring AFM domain boundaries aligned with the external magnetic field. The c-axis magnetization below $T_{Ho} \sim 5$ K shows that the FC magnetization becomes lower than the ZFC curve, which is explained as a ferrimagnetic-like coupling of magnetic moments in domain boundaries. We propose that this phenomenon is related either to the different temperature dependence of inequivalent Mn^{3+} and Ho^{3+} magnetic components that are oppositely oriented at AFM domain walls or to minor and major Ho^{3+} magnetic sublattices antiferromagnetically ordered at 34 and 5 K, respectively.

Acknowledgments

We would like to thank Professor Yuyi Xue for several useful discussions. This work was supported by the T L L Temple Foundation, the John J and Rebecca Moores Endowment, and the State of Texas through the Texas Center for Superconductivity at the University of Houston; and at Lawrence Berkeley Laboratory by the Director, Office of Science, Office of Basic Energy Sciences, Division of Materials Sciences and Engineering of the US Department of Energy under Contract No. DE-AC03-76SF00098.

References

[1] Smolenskii G A and Chupis I E 1982 *Sov. Phys.—Usp.* **25** 475
[2] Schmid H 1994 *Ferroelecrics* **162** 317
[3] Eerenstein W, Mathur N D and Scott J F 2006 *Nature* **442** 759
[4] Lottermoser T, Lonkai T, Amann U, Hohlwein D, Ihringer J and Fiebig M 2004 *Nature* **430** 541
[5] Fiebig M, Lottermoser T, Fröhlich D, Goltsev A V and Pisarev R V 2002 *Nature* **419** 818
[6] Hur N, Park S, Sharma P A, Ahn J S, Guha S and Cheong S W 2004 *Nature* **429** 392
[7] Lorenz B, Litvinchuk A P, Gospodinov M M and Chu C W 2004 *Phys. Rev. Lett.* **92** 087204
[8] Yen F, dela Cruz C, Lorenz B, Galstyan E, Sun Y Y, Gospodinov M and Chu C W 2007 *J. Mater. Res.* **22** 2163
[9] Lonkai T, Hohlwein D, Ihringer L and Prandl W 2002 *Appl. Phys.* A **74** 843
[10] Arlt G, Hennings D and de With G 1985 *J. Appl. Phys.* **58** 1619
[11] Fang T T, Hseih H L and Shiau F S 1993 *J. Am. Ceram. Soc.* **76** 1205
[12] Néel L 1961 *C. R. Acad. Sci. Paris* **252** 4075
[13] Gider S, Awschalom K K, Mann S and Chaparala M 1995 *Science* **268** 77
[14] Lorenz B, Yen F, Gospodinov M M and Chu C W 2005 *Phys. Rev.* B **71** 014438

[15] Martirosyan K S and Luss D 2005 *AIChE J.* **51** 2801
[16] Martirosyan K S and Luss D 2007 *Ind. Eng. Chem. Res.* **46** 1492
[17] Martirosyan K S, Chang L, Rantschler J, Khizroev S, Luss D and Litvinov D 2007 *IEEE Trans. Magn.* **43** 6
[18] Zhou J-S, Goodenough J B, Gallardo-Amores J M, Morán E, Alario-Franco M A and Caudillo R 2006 *Phys. Rev.* B **74** 014422
[19] Muñoz A, Alonso J A, Martinez-Lope M J, Casais M T, Martinez J L and Fernandez-Diaz M T 2001 *Chem. Mater.* **13** 1497
[20] Hennings D F K, Schreinmacher B and Schreinmacher H 1994 *J. Eur. Ceram. Soc.* **13** 81
[21] Sugie H, Iwata N and Kohn K 2002 *J. Phys. Soc. Japan* **71** 1558
[22] Kodama R H, Makhlouf S A and Berkowitz A E 1997 *Phys. Rev. Lett.* **79** 1393
[23] Bañdobre-Lopez M, Vázquez-Vázquez C, Rivas J and Lopez-Quintela M A 2003 *Nanotechnology* **14** 318
[24] Morrish A H 2001 *The Physical Principles of Magnetism* (New York: IEEE)
[25] Zysler R D, Winkler E, Vasquez Mansilla M and Fiorani D 2006 *Physica* B **384** 277
[26] Narsinga Rao G, Yao Y D and Chen J W 2005 *IEEE Trans. Magn.* **41** 3405
[27] Tomuta D G, Ramakrishnan S J, Nieuwenhuys G and Mydosh J A 2001 *J. Phys.: Condens. Matter* **13** 4543
[28] Muñoz A, Alonso J A, Martinez-Lope M J, Casais M T, Martinez J L and Fernandez-Diaz M T 2000 *Phys. Rev.* B **62** 9498
[29] Yen F, dela Cruz C, Lorenz B, Sun Y Y, Wang Y Q, Gospodinov M and Chu C W 2005 *Phys. Rev.* B **71** 180407(R)